# Minimizing Transmit Power for Coherent Communications in Wireless Sensor Networks With Finite-Rate Feedback

Antonio G. Marques, *Member, IEEE*, Xin Wang, *Member, IEEE*, and Georgios B. Giannakis, *Fellow, IEEE*

***Abstract*—We minimize average transmit power with finite-rate feedback for coherent communications in a wireless sensor network (WSN), where sensors communicate with a fusion center using adaptive modulation and coding over a wireless fading channel. By viewing the coherent WSN setup as a distributed space–time multiple-input single-output (MISO) system, we present optimal distributed beamforming and resource allocation strategies when the full (F-) channel state information at the transmitters (CSIT) is available through a feedback channel. We also develop optimal adaptive transmission policies and design optimal quantizers for the finite-rate feedback case where the sensors only have quantized (Q-) CSIT, or, each sensor has F-CSIT of its own link with the FC but only Q-CSIT of other sensors. Numerical results confirm that our novel finite-rate feedback-based strategies achieve near-optimal power savings based on even a small number of feedback bits.**

***Index Terms*—Multiple-input single-output (MISO) systems, nonlinear optimization, power efficiency, quantization, resource allocation, wireless sensor networks (WSNs).**

## I. Introduction

A WIRELESS sensor network (WSN) comprises a large number of spatially distributed signal processing devices (sensor nodes). In a number of application scenarios, WSN nodes are equipped with a nonrechargeable battery and thus have limited computing and communication capabilities. When properly programmed and networked, nodes in a WSN can cooperate to perform advanced signal processing tasks with unprecedented robustness and versatility, thus making WSN an attractive low-cost technology for a wide range of remote sensing and environmental monitoring applications [1]. One of the main objectives in current WSN research is to design power-efficient devices and algorithms to support different aspects of network operations [6]. Various power-efficient algorithms have been proposed for network coverage, medium access control protocols, decentralized estimation and routing; see e.g., [6], [19], [24], [23], and [2]. The WSN in many of these works includes a fusion center (FC) with which sensors are linked.

When these links are fading, communication performance across the WSN coverage area is severely degraded. A well-known approach to mitigate the adverse effects of fading relies on transmissions adapting to the *full* (F-) channel state information (CSI) [12], [10]. In practice, CSI at transmitters (CSIT) is typically acquired through a limited-rate feedback channel from the receiver, and thus, only *quantized* (Q-) CSIT is available [9]. This finite-rate feedback model is pragmatically affordable and is robust to channel estimation errors, feedback delay and jamming [13]. Adaptive transmissions and/or beamforming schemes based on Q-CSIT have been optimized for multiple-input multiple-output (MIMO) systems to maximize rate or receive-signal-to-noise-ratio (SNR), [16], [20], or, to minimize bit error rate (BER) [25]; as well as to optimize power efficiency for single-input single-output (SISO) and multiuser systems [18], [19].

This paper deals with a *distributed* multiple-input single-output (MISO) communication system in the *power-limited* regime of a WSN where sensor transmissions arrive coherently at the FC [3], [4]. Timing needed to ensure coherence is assumed to have been acquired using e.g., the low-complexity synchronization algorithm of [17]. Specifically, the sensors' average transmit power is minimized subject to average rate and BER constraints, based on three different types of CSIT:

i) F-CSIT where each channel realization is assumed available at each sensor;
ii) Q-CSIT where the sensors only have quantized knowledge of their links with the FC; and
iii) individual (I-) CSIT where each sensor has full knowledge of its own channel but only quantized knowledge of the other sensors' channels.

For these cases, we develop corresponding adaptive modulation/coding, power loading and beamforming strategies as well as the channel quantizers needed to form the required Q-CSIT as the solution of constrained optimization problems.

Manuscript received October 5, 2006; revised December 23, 2007. Published August 13, 2008. The associate editor coordinating the review of this manuscript and approving it for publication was Dr. Soren Holdt Jensen. Work in this paper was supported by the ARO Grant W911NF-05-1-0283 and was prepared through collaborative participation in the Communications and Networks Consortium sponsored by the U.S. Army Research Laboratory under the Collaborative Technology Alliance Program, Cooperative Agreement DAAD19-01-2-0011. The U.S. Government is authorized to reproduce and distribute reprints for Government purposes notwithstanding any copyright notation thereon. The work of A. G. Marques in this paper was partially supported by the C.A. Madrid Government Grant P-TIC-000223-0505. Parts of this paper were presented at the Asilomar Conference on Signals, Systems, and Computers, Pacific Grove, CA, October 2006, and the IEEE International Conference on Acoustics, Speech, and Signal Processing, Honolulu, HI, April 2007.

A. G. Marques is with the Department of Signal Theory and Communications, Rey Juan Carlos University, Fuenlabrada, Madrid 28943, Spain (e-mail: antonio.garcia.marques@urjc.es).

X. Wang is with the Department of Electrical Engineering, Florida Atlantic University, Boca Raton, FL 33431, USA (e-mail: xin.wang@fau.edu).

G. B. Giannakis is with the Department of Electrical and Computer Engineering, University of Minnesota, Minneapolis, MN 55455 USA (e-mail: georgios@ece.umn.edu).

Color versions of one or more of the figures in this paper are available online at http://ieeexplore.ieee.org.

Digital Object Identifier 10.1109/TSP.2008.921725

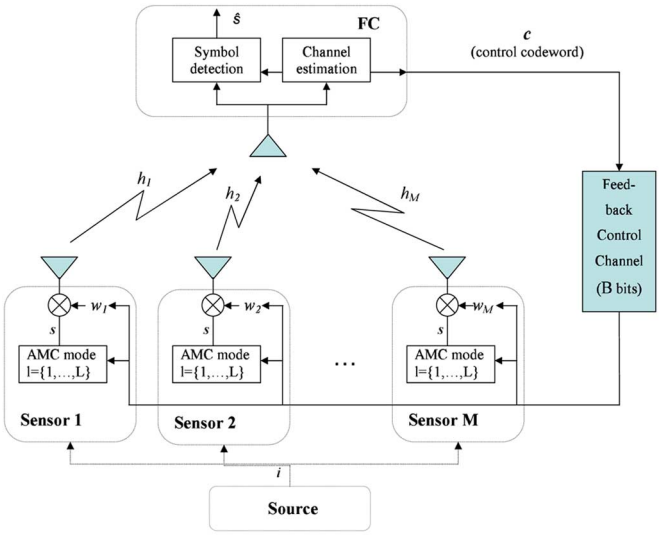


Fig. 1. System model.

The rest of the paper is organized as follows. After introducing modeling preliminaries in Section II, we derive in Section III optimal transmit-adaptation based on F-CSIT which provides fundamental limits and benchmarks the power efficiency based on Q-CSIT. Subsequently, we solve the optimal adaptation problem based on Q-CSIT in Section IV, while Section V deals with the optimal design based on I-CSIT. Simulated examples and comparisons are provided in Section VI, followed by concluding remarks.

*Notation:* We use boldface lower-case letters to denote column vectors, $^T$ to denote transposition, $^\dagger$ conjugate, $^{\mathcal{H}}$ conjugate transposition, and $||\cdot||$ the Euclidean norm. For a random variable $x$, $f_x(x)$ will denote its probability density function (PDF), and $F_x(x)$ its cumulative distribution function (CDF). Furthermore, $\mathcal{CN}(\mu,\sigma^2)$ will denote the complex-Gaussian distribution with mean $\mu$ and variance $\sigma^2$, $\lceil x \rceil$ the minimum integer $\geq x$, and $\mathbb{E}_x[\cdot]$ the expectation operator over $x$.

## II. Modeling Preliminaries

We consider a WSN setup where $M$ sensors indexed by $m \in \{1,\ldots,M\}$ wish to communicate an information message (say the value of a random variable they track or information they relay) to the FC; see Fig. 1. We assume that:

**(as1)** *the information is common to all sensors and arrives coherently at the FC.*

With $\{h_m\}_{m=1}^M$ denoting block fading channel coefficients between sensors and the FC, we further assume that:

**(as2)** $\{h_m\}_{m=1}^M$ *are independent and identically distributed (i.i.d.) according to a complex Gaussian distribution with zero mean and unit variance, i.e.,* $h_m \sim \mathcal{CN}(0,1)$*; and each block fading channel process* $h_m$ *is ergodic;*

**(as3)** *the FC feeds back to the sensors the CSI indexed by* $B$ *bits per channel realization, without error and with negligible delay.*

As in [3] and [4], synchronization in (as1) is assumed acquired using low-complexity synchronization algorithms; see, e.g., [17] and references therein. A setup where sensors have a common message to transmit as in (as1) fits a cooperative scenario where bits from a common source encoded with sufficiently powerful error control codes are relayed through distributed sensors to a destination. On the other hand, for WSNs deployed to perform an estimation task, common data across sensors can be safely assumed identical under any one of the following three operating conditions: (c1) sensors are located inside a small area and the information-bearing source is close enough so that errors in recovering the source data at the sensors can be deemed negligible; (c2) instead of multiple single-antenna sensors, we have a single multi-antenna sensor; or (c3) sensors exchange information to consent on the source. Besides providing mathematical tractability, (as2) can also hold under any one of aforementioned operating conditions (c1)–(c3). Extension to correlated channels is possible but is out of the scope of this work. Finally, (as3) can be easily guaranteed with sufficiently strong error control codes, since the feedback channel has typically low rate.

Given a pool of adaptive modulation and coding (AMC) pairs, we suppose that each sensor supports a finite number $L$ of AMC modes indexed by $l \in \{1,\ldots,L\}$, with each mode having constellation size $M_l$ and transmission rate $r_l := r_c \log_2(M_l)$, where $r_c$ denotes the coding rate. To guarantee quality of service, the rates $\{r_l\}_{l=1}^L$ must be delivered with a prescribed BER $\epsilon_0$. To mitigate the effects of fading, the sensors beamform their transmitted symbol. Since a MISO system has multiplexing gain one (see, e.g., [9 pp. 48]), the sensors encode one information-bearing symbol $s$ per channel use utilizing a common AMC mode. With this AMC mode, the $m$th sensor transmits $s$ multiplied by a complex (steering) weight $w_m$. Let $\mathbf{w} := [w_1,\ldots,w_M]^T$ denote the distributed beamforming vector and $\mathbf{h} := [h_1,\ldots,h_M]^T$ the fading MISO channel. The received symbol $y$ at the FC can be expressed as

$$y = \mathbf{w}^T\mathbf{h}s + v := ||\mathbf{w}||^2\mathbf{u}^T\mathbf{h}s + v \tag{1}$$

where $\mathbf{u} := \mathbf{w}/||\mathbf{w}||$, and $v$ denotes the additive white Gaussian noise (AWGN) with zero mean and variance $N_0$. Notice that both the phase and the modulus of $\mathbf{w}$ can be tuned to effect not only distributed beamforming but also power allocation per fading state $\mathbf{h}$. Letting $E_s$ denote the average energy per symbol, we can write the total transmit power and receive-SNR per symbol as

$$p := ||\mathbf{w}||^2 E_s = ||\mathbf{w}||^2 \tag{2}$$

$$\gamma := |\mathbf{w}^T\mathbf{h}|^2 \frac{E_s}{N_0} = p|\mathbf{u}^T\mathbf{h}|^2 \tag{3}$$

where for the last equality in (2) and (3) we have assumed without loss of generality that $E_s = N_0 = 1$. It follows from (3) that after beamforming, the MISO vector channel $\mathbf{h}$ in (1) is fully characterized by the equivalent SISO scalar channel with normalized power gain $g := |\mathbf{u}^T\mathbf{h}|^2$. The receive-SNR for the equivalent SISO system can be rewritten as $\gamma = pg$.

Let $\mathbf{c} = \mathbf{c}(\mathbf{h})$ denote the $B$-bit Q-CSI codeword that the FC feeds back to the sensors per (as3). Based on $\mathbf{c}(\mathbf{h})$, the sensors adapt their transmit-parameters to one of $N = 2^B$ prescribed modes specifying the transmission rate $r = r(\mathbf{c})$, transmit power $p = p(\mathbf{c})$ and beamforming vector $\mathbf{u} = \mathbf{u}(\mathbf{c})$.

Our goal is to optimally design the channel quantizer which yields $\mathbf{c}(\mathbf{h})$ based on which we wish to adapt $r = r(\mathbf{c}), p = p(\mathbf{c})$, and $\mathbf{u} = \mathbf{u}(\mathbf{c})$, so that the total average power transmitted by all sensors is minimized subject to average rate and BER requirements. To this end, we will first rely on F-CSIT which corresponds to setting $B = \infty$ in (as3).

## III. Solution Based on F-CSIT

In this section, we derive the optimal adaptive transmission policy based on F-CSIT to provide insight and benchmark the Q-CSIT based design of Section IV. For $B = \infty$, Q-CSIT becomes F-CSIT; i.e., $\mathbf{c}(\mathbf{h}) = \mathbf{h}$. Given $\mathbf{h}$, we wish to adapt the transmit power $p(\mathbf{h})$, rate $r(\mathbf{h})$ and beamforming vector $\mathbf{u}(\mathbf{h})$ to minimize the average transmit power subject to prescribed requirements on the average rate $(r_0)$ and BER $(\epsilon_0)$. As we show next, the adaptation of the beamformer can be performed separately from the power and rate adaptation without loss of optimality (w.l.o.o.). This allows us to tackle the original problem in two separate phases: first we solve for the optimal[1] adaptation of the beamformer $\mathbf{u}^*(\mathbf{h})$; next we introduce $\mathbf{u}^*(\mathbf{h})$ in the original problem and solve for the optimal power $p^*(\mathbf{h})$ and rate $r^*(\mathbf{h})$ adaptation.

### A. Optimal Distributed Beamformer

From (2) and (3) we recognize that the selection of $\mathbf{u}$ affects the scalar channel gain $g$. Since for any AMC mode the required transmit power $p = p(\mathbf{h})$ is monotonically decreasing w.r.t. $g$ (for any given $r_0$ and $\epsilon_0$), to minimize the transmit power we have to adapt $\mathbf{u} = \mathbf{u}(\mathbf{h})$ per channel realization $\mathbf{h}$ so that $g = |\mathbf{u}^T(\mathbf{h})\mathbf{h}|^2$ is maximized. The optimal unitary beamforming vector maximizing $|\mathbf{u}^T(\mathbf{h})\mathbf{h}|^2$, hence minimizing the required transmit power, is clearly (see, e.g., [10, Sec. 7.3.1])

$$\mathbf{u}^*(\mathbf{h}) = \mathbf{h}^\dagger/\|\mathbf{h}\| \tag{4}$$

and depends only on the channel phase, i.e., $\mathbf{u}^*(\mathbf{h}) = \mathbf{u}^*(\mathbf{h}/\|\mathbf{h}\|)$.

To proceed with the optimal rate and power allocation strategies, we need to characterize statistically the channel in (1) when beamforming is adapted as in (4). When $\mathbf{u}^*(\mathbf{h}) = \mathbf{h}^\dagger/\|\mathbf{h}\|, \forall \mathbf{h}$, the channel gain is

$$g = |\mathbf{u}^T(\mathbf{h})\mathbf{h}|^2 = \|\mathbf{h}\|^2. \tag{5}$$

As per (as2), $g$ adheres to a chi-squared distribution with PDF

$$f_g(g) = \frac{g^{M-1}\exp(-g)}{\Gamma(M)} \tag{6}$$

where $\Gamma(b,x) := \int_x^\infty t^{b-1}e^{-t}dt$ is the incomplete Gamma function and $\Gamma(b) := \Gamma(b,0)$. The corresponding CDF is

$$F_g(g) = \frac{\Gamma(M,g)}{\Gamma(M)}. \tag{7}$$

It is worth to recall that when optimal beamforming $\mathbf{u}^*(\mathbf{h})$ in (4) is implemented, the MISO channel in (1) is fully characterized by an equivalent SISO channel with power gain $g$ dictated by (5). This implies w.l.o.o. that solving for the optimal $r^*(\mathbf{h})$ and $p^*(\mathbf{h})$ is equivalent to finding the optimal $r^*(g)$ and $p^*(g)$. Notice that since $\mathbf{h}$ (and thus $g$) varies from one realization to the next, rate and power will be adapted across time in order to minimize the *average* transmit power under an *average* rate constraint $r_0$ (the requirement $\epsilon_0$ on BER will be automatically accounted for in the relationship between the power and the rate as we will see next).

### B. Optimal Rate and Power Allocation

We order the AMC modes such that $r_l < r_{l+1}\ \forall l > 1$ and let the first mode represent the inactive mode with zero rate and power $(r_1 = p_1 = 0)$. With $\epsilon(\cdot)$ denoting the instantaneous BER function, the minimum transmit power for the $l$th AMC mode to satisfy the BER requirement $\epsilon_0$ can be calculated by solving with respect to (w.r.t.) $p_l$ the equation

$$\epsilon(g, p_l, r_l) = \epsilon_0. \tag{8}$$

For $M$-ary quadrature amplitude modulation (QAM), the BER can be accurately approximated as[2] [11] (e.g., $\kappa_1 = 0.2, \kappa_2 = 1.5$ for uncoded transmissions)

$$\epsilon(g, p, r) = \kappa_1 \exp(-\kappa_2 gp/(2^r - 1)). \tag{9}$$

Substituting (9) into (8), the required power for the $l$th AMC mode can be expressed as

$$p_l(g, r_l, \epsilon_0) = \frac{(2^{r_l} - 1)}{g}\frac{\ln(\kappa_1/\epsilon_0)}{\kappa_2}. \tag{10}$$

With F-CSIT available, (10) shows that specifying the AMC mode determines not only the rate but also the power required to meet the prescribed $\epsilon_0$. Furthermore, it is easy to see that with $p_l, r_l$ given the range of $g$ can be divided into $L$ consecutive intervals $[\tau_l, \tau_{l+1})$ with $\tau_1 = 0$ and $\tau_{L+1} = \infty$, and the $l$th AMC mode will be chosen if $g \in [\tau_l, \tau_{l+1})$. Conversely, this means that once the intervals $[\tau_l, \tau_{l+1})$ are specified for $l = 1, \ldots, L$, the rate and power allocations will be

$$r(g) = r_l; \quad \text{if } g \in [\tau_l, \tau_{l+1}) \tag{11}$$

$$p(g, \epsilon_0) = \begin{cases} 0, & g \in [\tau_1, \tau_2) \\ \frac{(2^{r_l}-1)}{g}\frac{\ln(\kappa_1/\epsilon_0)}{\kappa_2}, & g \in [\tau_l, \tau_{l+1}), l > 1. \end{cases} \tag{12}$$

Letting $\boldsymbol{\tau} := [\tau_1, \ldots, \tau_{L+1}]^T$, (11) and (12) imply that to find the optimal rate and power allocations, we only need to search for the optimal $\boldsymbol{\tau}^*$ which solves the following constrained minimization problem:

$$\begin{cases} \min_{\boldsymbol{\tau}} \quad \bar{p}, \\ \text{where} \quad \bar{p} := \sum_{l=1}^{L}\int_{\tau_l}^{\tau_{l+1}} p_l(g, r_l, \epsilon_0) f_g(g) dg \\ \text{subject to :} \quad C1. \sum_{l=1}^{L}\int_{\tau_l}^{\tau_{l+1}} r_l f_g(g) dg \geq r_0 \\ \qquad\qquad\ C2.\ \tau_l \leq \tau_{l+1}\ \forall l \end{cases} \tag{13}$$

[1] Henceforth, $x^*$ will denote the optimal value of $x$.

[2] Extensions to modulation schemes other than M-QAM are also possible. By appropriately selecting $\kappa_1$ and $\kappa_2$, (9) can also be used to accommodate (un)coded transmissions as a BER upperbound based on the Chernoff bound [21].

where the average transmit power $\bar{p}$ in the objective and the average rate in $C1$ are calculated as the expectation of $p(g)$ and $r(g)$ over all the possible realizations of $g$. The set of constraints $C2$ ensures consistency of the intervals $[\tau_l, \tau_{l+1})$.

Let $\lambda$ denote the non-negative Lagrange multiplier associated with the rate constraint $C1$ and $\boldsymbol{\alpha} := [\alpha_1, \ldots, \alpha_L]^T$ the non-negative Lagrange multipliers associated with the $L$ constraints in $C2$. The Lagrangian of (13) is then given by

$$\mathcal{L}(\lambda, \boldsymbol{\alpha}, \boldsymbol{\tau}) = \sum_{l=1}^{L} \int_{\tau_l}^{\tau_{l+1}} p_l(g, r_l, \epsilon_0) f_g(g) dg - \lambda \left( \sum_{l=1}^{L} \int_{\tau_l}^{\tau_{l+1}} r_l f_g(g) dg - r_0 \right) + \sum_{l=1}^{L} \alpha_l (\tau_l - \tau_{l+1}). \quad (14)$$

At the optimum $\tau_l^*$ the necessary Karush–Kuhn–Tucker (KKT) condition is [7]

$$\frac{\partial \mathcal{L}(\lambda^*, \boldsymbol{\alpha}^*, \boldsymbol{\tau}^*)}{\partial \tau_l} = [p_{l-1}(\tau_l^*, r_{l-1}, \epsilon_0) - \lambda^* r_{l-1} - p_l(\tau_l^*, r_l, \epsilon_0) + \lambda^* r_l] f_g(\tau_l^*) - \alpha_{l-1}^* + \alpha_l^* = 0. \quad (15)$$

If all the constraints in $C2$ are slack, i.e., $\tau_l^* < \tau_{l+1}^*$, then $\alpha_l^* = 0, \forall l$. In this case, solving (15) w.r.t. $\tau_l^*$ yields for $l \in \{2, \ldots, L\}$ [cf. (10)]

$$\tau_l^* = \frac{(2^{r_l} - 2^{r_{l-1}})}{\lambda^* (r_l - r_{l-1})} \frac{\ln(\kappa_1/\epsilon_0)}{\kappa_2}. \quad (16)$$

Equation (16) expresses the optimal threshold $\tau_l^*$ in closed-form as a function of the Lagrange multiplier $\lambda^*$. Upon defining $f(x) := (2^x)\ln(\kappa_1/\epsilon_0)/(\lambda^* \kappa_2)$, we can rewrite (16) as $\tau_l^* = [f(r_l) - f(r_{l-1})]/(r_l - r_{l-1})$. As $\partial f(x)/\partial x = 2^x/x^3[\ln^2(2)x^2 - 2\ln(2)x + 2] > 0, \forall x > 0$, it is easy to see $\tau_l^* < \tau_{l+1}^*$. Therefore, the thresholds given by (16) indeed satisfy $\tau_l^* < \tau_{l+1}^*$ and thus they are the solutions to (15).

With $\tau_l^*$ specified by (16), $\lambda^*$ can be calculated to satisfy $C1$ using the following algorithm.

*Algorithm 1: Offline Power-Efficient Quantization (F-CSIT)*

- **(S1.0)** Let $\delta$ be a small tolerance level and initialize $\lambda$ with an arbitrary positive number.
- **(S1.1)** Calculate $\{\tau_l\}_{l=2}^L$ via (16).
- **(S1.2)** Using (7), calculate the average rate as $\bar{r} = \sum_{l=1}^{L} [F_g(\tau_{l+1}) - F_g(\tau_l)] r_l$, and check $C1$. If $|\bar{r} - r_0|/r_0 < \delta$ then *stop*; otherwise, calculate $\triangle\lambda := (\bar{r} - r_0)c$, update the multiplier as $\lambda = \lambda + \triangle\lambda$, and go to (S1.1). Parameter $c$ in the calculation of $\triangle\lambda$ is an adaptive penalty parameter that can be updated (per iteration) depending on convergence requirements.[3]

[3]The proposed updating scheme for $\lambda$ is based on the *method of multipliers* [5, Sec. 4.2].

Once $\lambda^*$ is obtained using Algorithm 1 (that is computed offline), $\{\tau_l^*\}_{l=2}^L$ and in turn the optimal rate and power allocations are determined after plugging (16) into (11) and (12).

### C. On-Line Feedback and Adaptation of Transmitters

Having obtained $\{\tau_l^*\}_{l=2}^L$, the following algorithm summarizes the online resource allocation steps the WSN has to execute per channel realization:

*Algorithm 2: Online Adaptation (F-CSIT)*

For each channel realization $\mathbf{h}$:

- **(S2.1)** The FC determines the index $l^*(\mathbf{h}) = l^*(g)$ of the interval $[\tau_l^*, \tau_{l+1}^*)$ the channel gain $g$ falls into, and broadcasts to the sensors the F-CSIT codeword $\mathbf{c}((\mathbf{h})) = [l^*(\mathbf{h}); \mathbf{h}]$.
- **(S2.2)** Each sensor $m$ transmits using the $l^*(\mathbf{h})$th AMC mode and the optimal steering weight [cf. (4) and (10)] $w_m^* = \sqrt{p_{l^*(\mathbf{h})}(g, r_{l^*(\mathbf{h})}, \epsilon_0)} h_m^\dagger / \|\mathbf{h}\|$.

Notice that even though each sensor can calculate $l^*(\mathbf{h})$ using only $\mathbf{h}$ of the feedback message, we also include $l^*(\mathbf{h})$ in $\mathbf{c}(\mathbf{h})$ for robustness. This augmented feedback codeword reduces the computational burden at each sensor and also avoids the feedback during the initialization phase needed for the sensors to acquire $\boldsymbol{\tau}^*$ (recall that knowledge of $\boldsymbol{\tau}^*$ is required to determine the optimal power allocation and AMC mode selection). With the insights gained from the F-CSIT based benchmark, we next derive the optimal adaptation schemes when only Q-CSIT is available.

## IV. Solution Based on Q-CSIT

In this section, power-efficient sensor transmission and quantization schemes are derived based on Q-CSIT fed back from the FC to the sensors. Per fading realization, the FC quantizes $\mathbf{h}$ to find separately the optimal $\mathbf{u}$ according to a quantizer $Q_u(\cdot)$, and the optimal AMC mode and $p$ according to a different quantizer $Q_t(\cdot)$. Concatenating the beamforming vector index $\mathbf{c}_u = Q_u(\mathbf{h})$ with the transmission mode index $\mathbf{c}_t = Q_t(\mathbf{h})$, the FC feeds back the $B$-bit Q-CSI codeword $\mathbf{c} = [\mathbf{c}_u; \mathbf{c}_t]$, where $B = B_u + B_t$, with $B_u := \text{length}(\mathbf{c}_u)$ and $B_t := \text{length}(\mathbf{c}_t)$. Based on this codeword $\mathbf{c}$, sensors adapt their transmissions and beamforming weights to minimize their total average transmit power.[4]

### A. Optimal Distributed Beamformer

With only $B_u$ bits available, the beamforming vector $\mathbf{u}$ is chosen from a finite set $\mathcal{U} := \{\mathbf{u}_i\}_{i=1}^{N_u}$, where $N_u = 2^{B_u}$. As

[4]Although $Q_u(\cdot), Q_t(\cdot)$, and pertinent adaptation schemes will be found as solution of optimization problems, in principle we cannot claim global optimality among all the possible Q-CSIT designs that utilize $B$ feedback bits. In Section VI, we simulate the performance of our design and compare it with a lower bound on all Q-CSIT designs. Simulations indicate that the gap from the bound is small even for small values of $B$ and thus demonstrate that our design exhibits near-optimal performance globally among all Q-CSIT designs.

with F-CSIT to minimize the transmit power, the optimal $\mathbf{u} \in \mathcal{U}$ maximizes the equivalent scalar channel gain in (3), i.e.,

$$\mathbf{u}^*(\mathbf{h}) = \arg\max_{\mathbf{u}\in\mathcal{U}} |\mathbf{u}^T\mathbf{h}|^2. \tag{17}$$

Codebooks $\mathcal{U}$ have been optimized for collocated MISO systems [20], [16], [22]. Under various criteria, optimal codebooks minimize the maximum correlation between codewords. Based on the Grassmanian line packing criterion, [16] further showed that minimization of the maximum correlation is equivalent to maximization of the minimum chordal distance which for two unitary complex vectors $\mathbf{a}$ and $\mathbf{b}$ is defined as [8]

$$d_{\text{ch}}(\mathbf{a},\mathbf{b}) := (1 - |\mathbf{a}^T\mathbf{b}|^2)^{\frac{1}{2}}. \tag{18}$$

In view of (18), the optimization in (17) can be expressed as

$$\mathbf{u}^*(\mathbf{h}) = \arg\min_{\mathbf{u}\in\mathcal{U}} d_{\text{ch}}\left(\mathbf{u}, \frac{\mathbf{h}}{\|\mathbf{h}\|}\right) \tag{19}$$

and the optimal codebook $\mathcal{U}^*$ as

$$\mathcal{U}^* = \max_{\{\mathbf{u}_i\}_{i=1}^{N_u}} \min_{\forall i\neq j} d_{\text{ch}}(\mathbf{u}_i,\mathbf{u}_j). \tag{20}$$

For arbitrary beamformer sizes $M$ and codebook sizes $N_u$, numerical solutions of (20) are available; see, e.g., [15]. With the optimal codebook $\mathcal{U}^*$ available to both the FC and the sensors, the Q-CSI and optimal beamforming vector are then determined as

$$\mathbf{c}_u = Q_u(\mathbf{h}) := \arg_i \min_{\mathbf{u}\in\mathcal{U}^*} \left\{ d_{\text{ch}}\left(\mathbf{u}, \frac{\mathbf{h}}{\|\mathbf{h}\|}\right)\right\} \tag{21}$$

$$\mathbf{u}^*(\mathbf{h}) = \mathbf{u}_{\mathbf{c}_u}. \tag{22}$$

*Remark 1:* Beamforming specified by (21) and (22) has been proved to be optimal if $N_u \geq M$. For detailed analysis on Q-CSIT based beamforming when $N_u < M$, we refer the reader to [22].

Let us now turn our attention to the statistical characterization of the equivalent channel when Q-CSIT is available. Recall that the gain of this equivalent channel with F-CSIT available is $g = \|\mathbf{h}\|^2$ for the optimal beamformer in (4). But with the Q-CSIT based optimal beamformer in (21)–(22), the equivalent channel gain becomes $\tilde{g} := g(1-z)$, where

$$z := \min_{\mathbf{u}\in\mathcal{U}^*} d^2_{\text{ch}}(\mathbf{u}, \mathbf{h}/\|\mathbf{h}\|) = d^2_{\text{ch}}(\mathbf{u}^*(\mathbf{h}), \mathbf{h}/\|\mathbf{h}\|) \tag{23}$$

can be interpreted as the channel gain loss due to quantization. This channel gain loss degrades the instantaneous receive-SNR to $\gamma := p\tilde{g}$.

Based on the union bound, the CDF of $z$ can be upper-bounded tightly as [26]

$$F_z(z) \leq \tilde{F}_z(z) = \begin{cases} N_u z^{M-1}, & 0 \leq z \leq z_{\max} \\ 1, & z \geq z_{\max} \end{cases} \tag{24}$$

where $z_{\max} := N_u^{-1/(M-1)}$. Because $g$ and $z$ are independent [cf. (as2)], using the approximation $F_z(z) \simeq \tilde{F}_z(z)$, we can obtain the CDF of $\tilde{g}$ as

$$\begin{aligned} F_{\tilde{g}}(x) &= \Pr\{g(1-z) < x\} \\ &= \int_{g=0}^{\frac{x}{1-z_{\max}}} \int_{z=\max(0,1-x/g)}^{z_{\max}} f_z(z)dz f_g(g)dg \\ &= \int_{g=0}^{x} \int_{z=0}^{z_{\max}} f_z(z)dz f_g(g)dg \\ &\quad + \int_{g=x}^{\frac{x}{1-z_{\max}}} \int_{z=1-x/g}^{z_{\max}} f_z(z)dz f_g(g)dg \\ &= \int_{g=0}^{x} [\tilde{F}_z(z_{\max}) - \tilde{F}_z(0)] f_g(g)dg \\ &\quad + \int_{g=x}^{\frac{x}{1-z_{\max}}} [\tilde{F}_z(z_{\max}) - \tilde{F}_z(0)] f_g(g)dg \\ &= 1 - \frac{\Gamma(M, x/(1-z_{\max}))}{\Gamma(M)} \\ &\quad - N\exp(-x)\left(1 - \frac{\Gamma(M, xz_{\max}/(1-z_{\max}))}{\Gamma(M)}\right). \end{aligned} \tag{25}$$

The PDF of $\tilde{g}$ can be in turn obtained as $\partial F_{\tilde{g}}(\tilde{g})/\partial\tilde{g}$, yielding

$$\begin{aligned} f_{\tilde{g}}(\tilde{g}) &= \frac{1}{\Gamma(M)}\left\{\exp\left(\frac{-\tilde{g}}{1-z_{\max}}\right)\frac{\tilde{g}^{M-1}}{(1-z_{\max})^M}\left(1 - N_u z_{\max}^M\right)\right. \\ &\quad \left. + N_u\exp(-\tilde{g})[\Gamma(M) - \Gamma(M, z_{\max}\tilde{g}/(1-z_{\max}))]\right\}. \end{aligned} \tag{26}$$

The scalar channel gain $\tilde{g}$ fully characterizes the MISO channel when the optimal beamformer in (21)–(22) is adopted. Based on the closed-form expressions (25) and (26), we next follow an approach similar to what we used when F-CSIT is available to analytically derive the optimal rate and power allocation based on Q-CSIT.

### B. Optimal Rate and Power and Allocation

When only finite-rate feedback is available, the FC needs to quantize $\tilde{g}$ using a finite number of regions. Towards this objective, identifying each quantization region with an AMC mode selection emerges as a natural first step. We consider $L$ different quantization regions $\{\mathcal{R}_l := [\tilde{\tau}_l, \tilde{\tau}_{l+1})\}_{l=1}^L$, and as with F-CSIT, we associate with them the vector of thresholds $\tilde{\boldsymbol{\tau}} := [\tilde{\tau}_1, \ldots, \tilde{\tau}_{L+1}]^T$.

The $l$th transmission mode is characterized by the rate–power pair $(r_l, \tilde{p}_l)$ in the quantization region $\mathcal{R}_l$ (see also [14] which deals with throughput maximization). While $r_l$ is fixed for a given AMC mode, we will select $\tilde{p}_l$ to satisfy the BER requirement. Clearly, the average BER $\tilde{\epsilon}_l$ for the region $\mathcal{R}_l$ can be obtained as the expected number of erroneous bits divided by the expected number of transmitted bits; i.e.,

$$\tilde{\epsilon}_l(\tilde{\tau}_l, \tilde{\tau}_{l+1}, \tilde{p}_l, r_l) := \frac{\mathbb{E}_{\tilde{g}\in[\tilde{\tau}_l,\tilde{\tau}_{l+1})}[r_l\epsilon(\tilde{g}, \tilde{p}_l, r_l)]}{\mathbb{E}_{\tilde{g}\in[\tilde{\tau}_l,\tilde{\tau}_{l+1})}[r_l]}. \tag{27}$$

To satisfy the overall BER requirement $\epsilon_0$, we set

$$\tilde{\epsilon}_l(\tilde{\tau}_l, \tilde{\tau}_{l+1}, \tilde{p}_l, r_l) = \epsilon_0 \quad \forall l. \tag{28}$$

It is easy to see that (28) reduces to (8) as $L \to \infty$ (F-CSIT case). Furthermore, substituting (27) into (28) yields

$$\varphi_\epsilon(\tilde{\tau}_l, \tilde{\tau}_{l+1}, \tilde{p}_l, r_l, \epsilon_0) := \int_{\tilde{\tau}_l}^{\tilde{\tau}_{l+1}} \epsilon(\tilde{g}, \tilde{p}_l, r_l) f_{\tilde{g}}(\tilde{g}) d\tilde{g} - \epsilon_0 \int_{\tilde{\tau}_l}^{\tilde{\tau}_{l+1}} f_{\tilde{g}}(\tilde{g}) d\tilde{g} = 0. \quad (29)$$

Using an analytical expression for $\varphi_\epsilon$ we derive in Appendix A, we can solve (29) for $\tilde{p}_l$. The same expression for $\varphi_\epsilon$ can be used to obtain $\tilde{\epsilon}_l$ in closed-form, and thus quantify the average BER for any given quantization. Solving (29) for $\tilde{p}_l$ can be easily carried out with a one-dimensional search. Letting $\tilde{p}_l(\tilde{\tau}_l, \tilde{\tau}_{l+1}, r_l, \epsilon_0)$ denote this solution, the rate and power allocation $\forall \tilde{g}$ can be expressed as [cf. (11) and (12)]

$$\tilde{r}(\tilde{g}) = r_l; \quad \text{if } \tilde{g} \in [\tilde{\tau}_l, \tilde{\tau}_{l+1}) \quad (30)$$

$$\tilde{p}(\tilde{g}, \epsilon_0) = \begin{cases} 0, & \tilde{g} \in [\tilde{\tau}_1, \tilde{\tau}_2) \\ \tilde{p}_l(\tilde{\tau}_l, \tilde{\tau}_{l+1}, r_l, \epsilon_0), & \tilde{g} \in [\tilde{\tau}_l, \tilde{\tau}_{l+1}), l > 1. \end{cases} \quad (31)$$

Now as in the F-CSIT case, finding the optimal rate and power allocations reduces to searching for the optimal thresholds $\tilde{\boldsymbol{\tau}}^*$. The corresponding optimization problem based on Q-CSIT is:

$$\begin{cases} \min_{\tilde{\boldsymbol{\tau}}} \quad \bar{p}, \\ \text{where} \quad \bar{p} := \sum_{l=1}^{L} \tilde{p}_l(\tilde{\tau}_l, \tilde{\tau}_{l+1}, r_l, \epsilon_0) \int_{\tilde{\tau}_l}^{\tilde{\tau}_{l+1}} f_{\tilde{g}}(\tilde{g}) d\tilde{g} \\ \text{subject to :} \quad C1. \sum_{l=1}^{L} r_l \int_{\tilde{\tau}_l}^{\tilde{\tau}_{l+1}} f_{\tilde{g}}(\tilde{g}) d\tilde{g} \geq r_0 \\ \qquad\qquad C2. \ \tilde{\tau}_l \leq \tilde{\tau}_{l+1} \quad \forall l \end{cases} \quad (32)$$

where both transmit power in the objective as well as transmit rate in $C1$ are averaged over all channel regions (quantization states). Notice that different from the F-CSIT based problem in (13), the loaded power here does not vary with the channel gain, but only with the region index (i.e., the power loading is fixed per AMC mode) and therefore it does not appear in the integrals. In fact, $\int_{\tilde{\tau}_l}^{\tilde{\tau}_{l+1}} f_{\tilde{g}}(\tilde{g}) d\tilde{g}$ can be interpreted either as the probability of falling into the $l$th quantization region or as the probability of selecting the $l$th AMC mode.

Next we use the KKT conditions to find $\tilde{\tau}_l^*$. Let $\tilde{\lambda}$ denote the Lagrange multiplier associated with the rate constraint $C1$ and $\tilde{\boldsymbol{\alpha}} := [\tilde{\alpha}_2, \ldots, \tilde{\alpha}_L]^T$ the Lagrange multipliers corresponding to $C2$. As in (16), with $\tilde{\boldsymbol{\alpha}} = \mathbf{0}$, the KKT condition at the optimal $\tilde{\tau}_l^*$ dictates

$$\frac{\partial \mathcal{L}(\tilde{\lambda}^*, \tilde{\boldsymbol{\tau}}^*)}{\partial \tau_l} = \Big[\tilde{p}_{l-1}\left(\tilde{\tau}_{l-1}^*, \tilde{\tau}_l^*, r_{l-1}, \epsilon_0\right) - \tilde{\lambda}^* r_{l-1} - \tilde{p}_l\left(\tilde{\tau}_l^*, \tilde{\tau}_{l+1}^*, r_l, \epsilon_0\right) + \tilde{\lambda}^* r_l\Big] f_{\tilde{g}}\left(\tilde{\tau}_l^*\right) + \frac{\partial \tilde{p}_{l-1}}{\partial \tilde{\tau}_l}\left(\tilde{\tau}_{l-1}^*, \tilde{\tau}_l^*, r_{l-1}, \epsilon_0\right) \int_{\tilde{\tau}_{l-1}^*}^{\tilde{\tau}_l^*} f_{\tilde{g}}(\tilde{g}) d\tilde{g} + \frac{\partial \tilde{p}_l}{\partial \tilde{\tau}_l}\left(\tilde{\tau}_l^*, \tilde{\tau}_{l+1}^*, r_l, \epsilon_0\right) \int_{\tilde{\tau}_l^*}^{\tilde{\tau}_{l+1}^*} f_{\tilde{g}}(\tilde{g}) d\tilde{g} = 0. \quad (33)$$

Notice that using the CDF in (25), we have $\int_{\tilde{\tau}_l^*}^{\tilde{\tau}_{l+1}^*} f_{\tilde{g}}(\tilde{g}) d\tilde{g} = F_{\tilde{g}}(\tilde{\tau}_{l+1}^*) - F_{\tilde{g}}(\tilde{\tau}_l^*)$.

Since $\tilde{p}_l(\tilde{\tau}_{l-1}^*, \tilde{\tau}_l^*, r_{l-1}, \epsilon_0)$ is an implicit function [cf. (29)], to calculate $\partial \tilde{p}_l / \partial \tau_l$ we rely on the implicit differentiation theorem: $d\varphi_\epsilon = (\partial \varphi_\epsilon / \partial x) dx + (\partial \varphi_\epsilon / \partial y)(\partial y / \partial x) dx = 0$, which yields $(\partial y / \partial x) = (-\partial \varphi_\epsilon / \partial x) / (\partial \varphi_\epsilon / \partial y)$. Therefore, $\forall l \in \{2, \ldots, L\}$ and $\forall i \in \{1, \ldots, L\}$ we have

$$\frac{\partial \tilde{p}_i}{\partial \tilde{\tau}_l}(\tilde{\tau}_i, \tilde{\tau}_{i+1}, r_i, \epsilon_0) = \begin{cases} -\frac{[-\epsilon(\tilde{\tau}_l, \tilde{p}_i, r_l) + \epsilon_0] f_{\tilde{g}}(\tilde{\tau}_l)}{\int_{\tilde{\tau}_i}^{\tilde{\tau}_{i+1}} [\partial \epsilon(\tilde{g}, \tilde{p}_i, r_l)/\partial p] f_{\tilde{g}}(\tilde{g}) d\tilde{g}}, & i = l; \\ \frac{[-\epsilon(\tilde{\tau}_l, \tilde{p}_i, r_{l-1}) + \epsilon_0] f_{\tilde{g}}(\tilde{\tau}_l)}{\int_{\tilde{\tau}_i}^{\tilde{\tau}_{i+1}} [\partial \epsilon(\tilde{g}, \tilde{p}_i, r_{l-1})/\partial p] f_{\tilde{g}}(\tilde{g}) d\tilde{g}}, & i = l-1; \\ 0, & \text{otherwise.} \end{cases} \quad (34)$$

The denominators in (34) can be evaluated analytically (see Appendix B).

Different from the F-CSIT setup, we cannot guarantee that the optimal thresholds calculated from (33) always satisfy $\tilde{\tau}_l^* < \tilde{\tau}_{l+1}^*, \forall l$. If by solving (33) we obtain $\tilde{\tau}_l^* \geq \tilde{\tau}_{l+1}^*$, $C2$ is not slack, $\tilde{\alpha}_l^* > 0$, and (33) does not hold. In this case, since the KKT conditions also impose that $\tilde{\alpha}_l^*(\tilde{\tau}_l^* - \tilde{\tau}_{l+1}^*) = 0$, the optimal solution should yield $\tilde{\tau}_l^* = \tilde{\tau}_{l+1}^*$, and thus the $l$th mode should be removed from consideration. This implies that we need to check the feasibility of the solution obtained from (33). If solving (33) yields $\tilde{\tau}_l^* \geq \tilde{\tau}_{l+1}^*$ for a given $l$, we then need to remove this $l$th mode from the AMC pool and re-solve (33) for the remaining modes. Notice that calculating the optimal $\tilde{\tau}_l^*$ here depends not only on $\tilde{\lambda}^*$ but also on the previous $\tilde{\tau}_{l-1}^*$ and the next $\tilde{\tau}_{l+1}^*$. This prevents one from obtaining a closed-form expression for $\tilde{\tau}_l^*$. However, since closed-form expressions for all the terms in (33) are available, $\tilde{\tau}_l^*$ can be obtained numerically using a two-dimensional search which is computationally affordable.

*Algorithm 3: Offline Power-Efficient Quantization (Q-CSIT)*

- **(S3.0)** Let $\delta$ denote a small tolerance, $\varepsilon$ a small step size, and $\tilde{\tau}_L^{\max} > 0$ the maximum value for the highest quantization threshold (e.g., a value bringing the probability of the highest region close to 0).
- **(S3.1)** Initialize $\tilde{\lambda}$ with a small positive number and set $\tilde{\tau}_L = \tilde{\tau}_L^{\max}$; then calculate $\{\tilde{\tau}_l\}_{l=2}^L$ by solving (33). If $C2$ is not satisfied for some $\tau_l$, set $\tau_l = \tau_{l+1}$. If the obtained solution is feasible, go to (S3.2); otherwise decrease $\tilde{\tau}_L = \tilde{\tau}_L - \varepsilon$ and repeat (S3.1).
- **(S3.2)** Based on the closed-form in (25), calculate the average rate $\bar{r} = \sum_{l=1}^{L} [F_{\tilde{g}}(\tilde{\tau}_{l+1}) - F_{\tilde{g}}(\tilde{\tau}_l)] r_l$. Check $C1$ and if $|\bar{r} - r_0|/r_0 < \delta$ then *stop*; otherwise, calculate $\triangle\tilde{\lambda} := (\bar{r} - r_0) c$ using a small positive adaptive constant $c$, update the multiplier to $\tilde{\lambda} = \tilde{\lambda} + \triangle\tilde{\lambda}$, and go back to (S3.1).

Notice that the main computational burden in Algorithm 3 pertains to the calculation of the optimal thresholds in step (S3.1), which requires a two-dimensional search. Once the optimal $\tilde{\lambda}^*$ as well as $\{\tilde{\tau}_l^*\}_{l=2}^L$ are calculated, the optimal quantizer $Q_t(\cdot)$ can be readily determined as

$$\mathbf{c}_t = Q_t(\mathbf{h}) := \arg_i \left\{ g\left[1 - \min_{\mathbf{u} \in \mathcal{U}} d_{\text{ch}}^2(\mathbf{u}, \mathbf{h}/\|\mathbf{h}\|)\right] \in [\tilde{\tau}_i, \tilde{\tau}_{i+1}) \right\}. \quad (35)$$

With the AMC mode index $\mathbf{c}_t$ given by (35), the optimal rate and power allocation are obtained via (30) and (31).

### C. On-Line Feedback and Adaptation of Transmitters

Based on the optimal beamforming and resource allocation policy, we outline next the online algorithm executed by the FC and the sensors per channel realization.

*Algorithm 4: Online Adaptation (Q-CSIT)*

For each channel realization $\mathbf{h}$:

- **(S4.1)** The FC obtains $\mathbf{c}_u = Q_u(\mathbf{h})$ and $\mathbf{c}_t = Q_t(\mathbf{h})$ using, respectively, (21) and (35), and broadcasts the aggregate codeword $\mathbf{c} = [\mathbf{c}_u; \mathbf{c}_t]$ to the sensors.
- **(S4.2)** Each sensor $m$ transmits using the $m$th entry of the optimal beamforming vector indexed by $\mathbf{c}_u$, and loads the optimal power and rate allocation indexed by $\mathbf{c}_t$.

Notice that the optimal beamforming and resource allocation configurations must be available to both the FC and sensors during the initialization phase. In step (S4.2) the optimal transmit power $\tilde{p}^*_{\mathbf{c}_t}$ corresponding to $\mathbf{c}_t$ is calculated at the sensors by solving (29). This means that the sensors must know the optimal thresholds $\{\tilde{\tau}^*_l\}_{l=2}^L$ (i.e., the FC must broadcast them during the WSN deployment). To reduce the computational load at the sensors, an alternative is to let the FC calculate and feed back $\{\tilde{p}^*_l\}_{l=2}^L$ to the sensors during the initialization phase.

## V. Solution Based on I-CSIT

So far, we derived optimal adaptive transmission strategies based on F-CSIT where sensors perfectly know the vector channel $\mathbf{h}$, and based on Q-CSIT where sensors have available a quantized version of $\mathbf{h}$. In both cases, CSIT was obtained through feedback from the FC. However, for time-division duplex (TDD) systems, each sensor $m$ can acquire $h_m$ via pilot-based channel estimation during the symmetric reverse transmission. This motivates analysis of what we call individual (I-) CSIT scenario, where each sensor $m$ has full knowledge of $h_m$, but only finite-rate is available for CSI feedback.

### A. Optimal Distributed Beamforming

The adaptation in this case is similar to the one based on F-CSIT. When F-CSIT is available, (4) states that the optimal beamforming weight at $m$th sensor is $u^*_m(h) = h^\dagger_m/||\mathbf{h}||$. On the other hand when only I-CSIT is available, sensor $m$ has access to $h^\dagger_m$ but the value of $||\mathbf{h}||$ is unknown. To bypass this difficulty we define scaled beamformer and power variables as $\mathbf{v} := ||\mathbf{h}||\mathbf{u}$ and $\rho := p/||\mathbf{h}||^2$, respectively, so that $\mathbf{w} = \sqrt{\rho}\mathbf{v}$. Now the $m$th entry of the optimal $\mathbf{v}^*(\mathbf{h}) = \mathbf{h}^\dagger$ is $v^*_m(\mathbf{h}) = h^\dagger_m$, which requires only I-CSIT. The receive-SNR after optimal beamforming based on I-CSIT is $\gamma = \rho g^2 = pg$, where $g$ corresponds to the equivalent SISO channel gain in (5) and has PDF and CDF given by (6) and (7), respectively.

### B. Optimal Rate and Power Quantization and Allocation

Given I-CSIT, the optimal (scaled) beamformer is $\mathbf{v}^*(\mathbf{h})$. To construct the entire steering vector $\mathbf{w}(\mathbf{h})$, the sensors need also the (scaled) transmit power $\rho(\mathbf{h}) = p(\mathbf{h})/||\mathbf{h}||^2$ (or equivalently $\rho(g) := p(g)/g$), which requires knowledge of $||\mathbf{h}||$ and therefore depends on all the individual channels $h_m$. With finite-rate feedback, again the FC quantizes the channel gain $g$ using a finite number of regions. Similar to Q-CSIT, the domain of $g$ is partitioned into $L$ different quantization regions $\{\mathcal{R}_l := [\tilde{\tau}_l, \tilde{\tau}_{l+1})\}_{l=1}^L$ so that the $l$th AMC mode is employed by the sensors when $g \in \mathcal{R}_l$. Different from Q-CSIT, now the $l$th AMC mode is characterized by the rate–power pair $(r_l, \tilde{\rho}_l)$, where $\tilde{\rho}_l$ is fixed per region and must be selected to satisfy the BER requirement $\epsilon_0$. Upon defining

$$\psi_\epsilon(\tilde{\tau}_l, \tilde{\tau}_{l+1}, \tilde{\rho}_l, r_l, \epsilon_0) := \int_{\tilde{\tau}_l}^{\tilde{\tau}_{l+1}} \epsilon(g, \tilde{\rho}_l g, r_l) f_g(g) dg - \epsilon_0 \int_{\tilde{\tau}_l}^{\tilde{\tau}_{l+1}} f_g(g) dg \quad (36)$$

and arguing as in (27)–(35), it follows that a $\tilde{\rho}_l$ satisfying the prescribed BER (denoted by $\tilde{\rho}_l(\tilde{\tau}_l, \tilde{\tau}_{l+1}, r_l, \epsilon_0)$) should solve $\psi_\epsilon(\tilde{\tau}_l, \tilde{\tau}_{l+1}, \tilde{\rho}_l, r_l, \epsilon_0) = 0$. Unlike what we had in the Q-CSIT case for $\varphi_\epsilon$, no closed-form expression is available for $\psi_\epsilon$. However, relying on the fact that $\epsilon(g, \tilde{\rho}_l g, r_l)$ is monotonically decreasing w.r.t. to $\tilde{\rho}_l$, the root $\tilde{\rho}_l(\tilde{\tau}_l, \tilde{\tau}_{l+1}, r_l, \epsilon_0)$ can still be efficiently obtained via one-dimensional search.

We can now proceed to optimize resource allocation based on I-CSIT. Given $\tilde{\rho}_l(\tilde{\tau}_l, \tilde{\tau}_{l+1}, r_l, \epsilon_0)$ and a realization $\mathbf{h}$, the transmit power when the $l$th AMC mode is selected can be found as $p(\mathbf{h}) = ||\mathbf{h}||^2 \tilde{\rho}_l(\tilde{\tau}_l, \tilde{\tau}_{l+1}, r_l, \epsilon_0) = g\tilde{\rho}_l(\tilde{\tau}_l, \tilde{\tau}_{l+1}, r_l, \epsilon_0) = p(g)$. To find the optimal quantization thresholds $\tilde{\boldsymbol{\tau}}^* := [\tilde{\tau}^*_1, \ldots, \tilde{\tau}^*_{L+1}]^T$ minimizing the average transmit power, we need to solve

$$\begin{cases} \min_{\tilde{\boldsymbol{\tau}}} \quad \bar{p}, \\ \text{where } \bar{p} := \sum_{l=1}^L \tilde{\rho}_l(\tilde{\tau}_l, \tilde{\tau}_{l+1}, r_l, \epsilon_0) \int_{\tilde{\tau}_l}^{\tilde{\tau}_{l+1}} g f_g(g) dg \\ \text{subject to: } C1. \sum_{l=1}^L r_l \int_{\tilde{\tau}_l}^{\tilde{\tau}_{l+1}} f_g(g) dg \geq r_0 \\ \qquad\qquad C2. \ \tilde{\tau}_l \leq \tilde{\tau}_{l+1} \quad \forall l. \end{cases} \quad (37)$$

Letting $\tilde{\lambda}$ denote the Lagrange multiplier associated with $C1$ and assuming all the constraints in $C2$ are satisfied with strict inequality, the KKT condition for the optimal $\tilde{\tau}^*_l$ yields

$$\begin{aligned} \frac{\partial \mathcal{L}(\tilde{\lambda}^*, \tilde{\boldsymbol{\tau}}^*)}{\partial \tau_l} = & \Big[\tilde{\tau}^*_l \tilde{\rho}_{l-1}\left(\tilde{\tau}^*_{l-1}, \tilde{\tau}^*_l, r_{l-1}, \epsilon_0\right) - \tilde{\lambda}^* r_{l-1} \\ & - \tilde{\tau}^*_l \tilde{\rho}_l\left(\tilde{\tau}^*_l, \tilde{\tau}^*_{l+1}, r_l, \epsilon_0\right) + \tilde{\lambda}^* r_l\Big] f_g(\tilde{\tau}^*_l) \\ & + \frac{\partial \tilde{\rho}_{l-1}}{\partial \tilde{\tau}_l}\left(\tilde{\tau}_i, \tilde{\tau}_{i+1}, r_i, \epsilon_0\right) \int_{\tilde{\tau}^*_{l-1}}^{\tilde{\tau}^*_l} g f_g(g) dg \\ & + \frac{\partial \tilde{\rho}_l}{\partial \tilde{\tau}_l}(\tilde{\tau}_i, \tilde{\tau}_{i+1}, r_i, \epsilon_0) \int_{\tilde{\tau}^*_l}^{\tilde{\tau}^*_{l+1}} g f_g(g) dg = 0 \end{aligned} \quad (38)$$

where $\int_a^b g f_g(g)dg = [\Gamma(M+1,a) - \Gamma(M+1,b)]/\Gamma(M)$; and $\partial\tilde{\rho}_i/\partial\tilde{\tau}_l, \forall l \in [2,L], \forall i \in [1,L]$, can be obtained through implicit differentiation as

$$\frac{\partial\tilde{\rho}_i}{\partial\tilde{\tau}_l}(\tilde{\tau}_i,\tilde{\tau}_{i+1},r_i,\epsilon_0) = \begin{cases} -\frac{[-\epsilon(\tilde{\tau}_l,\tilde{\tau}_l\tilde{\rho}_i,r_l)+\epsilon_0]f_g(\tilde{\tau}_l)}{\int_{\tilde{\tau}_i}^{\tilde{\tau}_{i+1}}[\partial\epsilon(g,g\tilde{\rho}_i,r_l)/\partial p]gf_g(g)dg}, & i=l \\ \frac{[-\epsilon(\tilde{\tau}_l,\tilde{\tau}_l\tilde{\rho}_i,r_{l-1})+\epsilon_0]f_g(\tilde{\tau}_l)}{\int_{\tilde{\tau}_i}^{\tilde{\tau}_{i+1}}[\partial\epsilon(g,g\tilde{\rho}_i,r_{l-1})/\partial p]gf_g(g)dg}, & i=l-1 \\ 0, & \text{otherwise.} \end{cases} \quad (39)$$

Noticing the similarity between (38) and (33), we can readily devise the counterpart of Algorithm 3 to compute $\tilde{\lambda}^*$ and $\tilde{\boldsymbol{\tau}}^*$ offline.

### C. On-Line Feedback and Adaptation of Transmitters

Once the optimal thresholds $\tilde{\boldsymbol{\tau}}^*$ are obtained, the corresponding $\tilde{\rho}_l(\tilde{\tau}_l^*,\tilde{\tau}_{l+1}^*,r_l,\epsilon_0)$ can be computed at both the FC and the sensors, which then implement the following online algorithm to adapt their transmissions per channel realization:

*Algorithm 5: Online Channel Adaptation (I-CSIT)*

For each channel realization $\mathbf{h}$:

- **(S5.1)** The FC finds $l^*(\mathbf{h}) = l^*(g) = \arg_l\{g \in [\tilde{\tau}_l^*,\tilde{\tau}_{l+1}^*)\}$, and broadcasts $\mathbf{c} = [l^*(\mathbf{h})]$ to all sensors.
- **(S5.2)** Each sensor $m$ transmits the common symbol $s$ using the $l^*(\mathbf{h})$th AMC mode and steering weigh $w_m^* = \sqrt{\rho_{l^*(\mathbf{h})}(\tilde{\tau}_{l^*(\mathbf{h})}^*,\tilde{\tau}_{l^*(\mathbf{h})+1}^*,r_{l^*(\mathbf{h})},\epsilon_0)}h_m^\dagger$.

Notice that since the beamformer based on I-CSIT does not require feedback from the FC, we only need $B = \log_2(L)$ bits for CSI feedback, which may be significantly less than $B = \log_2(L+N_u)$ bits required to feed back the Q-CSIT, especially when $N_u$ is large.

## VI. Simulations

In this section, we present numerical examples to assess the transmit power consumed by the sensors when F-CSIT, Q-CSIT or I-CSIT is available. The energy per symbol, system bandwidth and AWGN power spectral density are selected to satisfy $E_s/N_0 = 1$. The simple cases tested include four sensors[5] with fading links adhering to (as1). Unless otherwise specified, we suppose that each sensor supports three active $M$-ary QAM uncoded modes: 2-QAM, 8-QAM and 32-QAM plus the inactive state; i.e., the transmission rates of AMC modes are: $r_l = 0,1,3,5$ bits per symbol. In all simulations, we set the BER requirement to $\epsilon_0 = 10^{-3}$ and wherever applicable, the codebook of beamforming vector has size $N_u = 16$.

[5]This setup is reasonable for, e.g., a WSN organized in clusters where the role of the FC is played by a cluster-head and only a few sensors are awake per cluster to minimize power consumption.

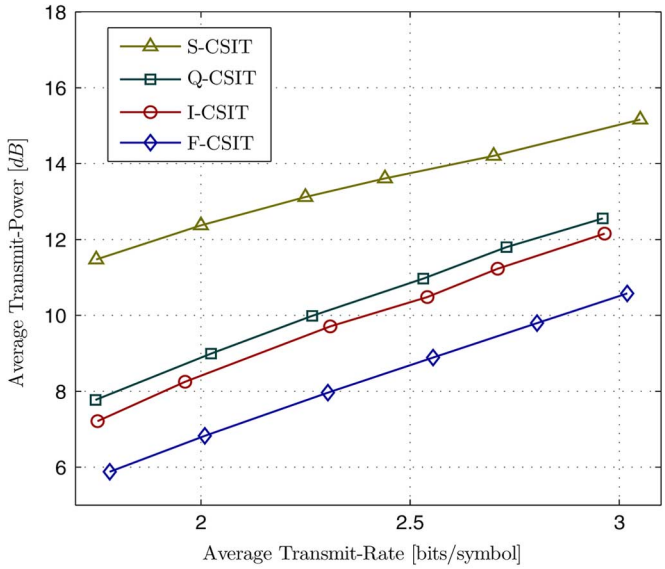


Fig. 2. Total transmit power versus total transmit rate for different CSIT scenarios ($M = 4, L = 4, N_u = 16$).

*Test Case 1 (Comparison of Transmit-Power Consumption):* For variable rate requirements, Fig. 2 shows the average normalized transmit power per symbol (in dB) achieved by the optimal adaptation policies based on: (i) F-CSIT, (ii) Q-CSIT, (iii) I-CSIT, and (iv) spatial (S-) CSIT. In the fourth S-CSIT case, we consider for comparison and illustration purposes that the sensors implement optimal spatial beamforming based on F-CSIT but do not implement temporal power allocation across time.

From Fig. 2, we have the following interesting observations: (i) both Q-CSIT and I-CSIT based strategies can achieve power efficiency close to the optimal F-CSIT based one; (ii) the Q-CSIT based and the I-CSIT based policies yield almost identical performance; (iii) the gap (in dB) between limited-rate feedback based policies and the optimal F-CSIT based one remains almost constant for different rate requirements; and, (iv) both Q-CSIT and I-CSIT based strategies clearly outperform the optimal S-CSIT scheme although the latter requires F-CSIT while the former only require of few bits of feedback.

To test the importance of feedback on power efficiency, we compare the power consumption by the optimal F-CSIT based policy and that of an open-loop system without feedback. As shown in Table I, the power consumed by the open-loop design is 20–25 dB higher than that of the closed-loop design based on F-CSIT. As expected, CSI can largely reduce power requirements, and thus considerably increase the *lifespan* of the WSN.

*Test Case 2 (Power Consumption for Different Scenarios):* Numerical results assessing the performance of F-CSIT, Q-CSIT, I-CSIT and S-CSIT based schemes over a wide range of parameter values are summarized in Table II. The simulation results confirm: i) the near optimality of Q-CSIT and I-CSIT based policies, and ii) the significant loss in power performance that the S-CSIT based system suffers from because it does not exploit the temporal diversity of the fading channel.

*Test Case 3 (Characterizing the Optimum Solution):* To gain more insights, Table III lists the optimal quantization and resource allocation for the three forms of CSIT. Recall that in the

TABLE I
AVERAGE TRANSMIT-POWER (IN dB) FOR OPEN-LOOP AND CLOSED-LOOP SYSTEMS AS $r_0$ VARIES

| $r_0$ | 1.75 | 2 | 2.25 | 2.5 | 2.75 | 3 |
|---|---|---|---|---|---|---|
| Closed-loop (F-CSIT) | 5.8 | 6.8 | 8.0 | 8.6 | 9.8 | 10.6 |
| Open-loop | 28.4 | 29.34 | 30.1 | 30.5 | 31.1 | 31.8 |

TABLE II
AVERAGE TRANSMIT POWER (IN dB) FOR (F, I, Q, AND S)-CSIT SCHEMES. (REFERENCE CASE: $M = 4, r_0 = 2.5, \epsilon_0 = 10^{-3}, L = 4, r_l = [0, 1, 3, 5], N_u = 16, E_s/N_0 = 1$; IN OTHER CASES, ONLY ONE INDICATED PARAMETER IS CHANGED W.R.T. THE REFERENCE CASE)

| CASE | F-CSIT | I-CSIT | Q-CSIT | S-CSIT |
|---|---|---|---|---|
| Reference Case | 8.6 | 10.2 | 10.7 | 13.8 |
| $M = 6$ | 5.0 | 6.5 | 6.9 | 11.2 |
| $E_s/N_0 = 3$ | 3.9 | 5.4 | 5.9 | 9.1 |
| $\epsilon_0 = 10^{-4}$ | 10.1 | 11.9 | 12.1 | 16.7 |
| $L = 6$ | 8.5 | 9.4 | 9.8 | 13.8 |
| $r_l = [0, 1, 2.6, 4]$ | 8.7 | 10.2 | 10.5 | 13.2 |

F-CSIT and I-CSIT based solutions the thresholds pertain to the channel gain $g$ whereas in the Q-CSIT solution they pertain to $\tilde{g} < g$.

It can be seen that in all closed-loop systems, the AMC mode with lower transmission-rate consumes the smallest average transmit power. We also observe that the optimal solutions try to equalize the power price per bit in all quantization regions. It turns out that for all cases the most likely AMC mode is the third one whose transmission rate ($r_3 = 3$) is the closest to the required rate $r_0 = 2.5$. This fact is more pronounced in the F-CSIT case where the optimal allocation allows adaptation of the transmit power per AMC mode and thus, reduces the need for adapting the rate. Interestingly, the thresholds are noticeably different for the three cases (recall that to fairly gauge the Q-CSIT case, we should use the equivalent thresholds pertaining to $g$, which are slightly larger than those for $\tilde{g}$ shown in Table III). These discrepancies are due to the difference in the SNR at the FC. Specifically, the receive-SNR is i) constant in the F-CSIT solution where $\gamma = p_l(g)g$ with $p_l(g)$ proportional to $1/g$; ii) proportional to $\tilde{g}$ in the Q-CSIT solution where $\gamma = \tilde{p}_l\tilde{g}$ with $\tilde{p}_l$ constant; and iii) proportional to $g^2$ in the I-CSIT solution where $\gamma = \tilde{\rho}_l g^2$ with $\tilde{\rho}_l$ constant. This also implies that the I-CSIT solution is very sensitive to small channel gains and, thus, it sets the threshold of the first active region to a relatively high value.

*Test Case 4 (Effect of the Number of Feedback Bits):* We have seen that with $L = 4$ (three active AMC modes) and $N_u = 16$, the Q-CSIT and I-CSIT based solutions yield power efficiency close to the optimal F-CSIT benchmark. This is achieved using $\lceil \log_2(4) + \log_2(16) \rceil = 6$ and $\lceil \log_2(4) \rceil = 2$ bits per channel realization for Q-CSIT and I-CSIT, respectively. Next, we analyze how the number of feedback bits affects the performance.

We first study the impact of varying the number of supported AMC modes. Table IV lists the total power cost in the F-CSIT, I-CSIT and Q-CSIT cases for different $L$ values. (When $L = 1$, the sensors only support one AMC mode which does not require feedback; whereas for all the remaining cases, sensors support $L - 1$ active AMC modes plus an inactive mode indexed by feeding back $\lceil \log_2(L) \rceil$ bits.) Recall that in the Q-CSIT based design, we assume that $N_u = 16$ beamforming modes can be employed. As $L$ increases, we observe that i) the power consumption decreases for all solutions, ii) the power-gap of the Q-CSIT and I-CSIT based systems from the F-CSIT benchmark also decreases, and iii) the first and second increments of $L$ bring the largest power savings. Notice also that the power consumed by the Q-CSIT solution exceeds that of the F-CSIT based system even as $L \to \infty$ when the former only relies on a beamforming codebook of finite size.

We next gauge the effect of varying $N_u$ in the Q-CSIT case. Fig. 3 plots the average transmit power versus the number of feedback bits $\log_2(N_u)$. For comparison, we also depict the transmit power for the corresponding I-CSIT and F-CSIT based solutions. Again the power consumption decreases as $N_u$ increases, while the reduction for each additional bit decreases. Note that as $N_u = \infty, \tilde{g} = g$, and thus only power quantization is implemented. Interestingly, we observe that when $N_u$ is large, the Q-CSIT based system outperforms the I-CSIT based one. As we already mentioned, divergence of the solutions in these two cases is due to the fact that quantizing the different variables ($p$ and $\rho = p/\|\mathbf{h}\|^2$) results in different optimal quantization designs. Intuitively, the advantage of Q-CSIT can be explained because variations in receive-SNR are less pronounced in the Q-CSIT solution ($g$ versus $g^2$) and this results in an optimal policy closer to the F-CSIT benchmark. However, it is worth to reiterate that the adaptation based on Q-CSIT requires more feedback bits than the one based on I-CSIT, especially when the Q-CSIT solution outperforms the I-CSIT one; i.e., when $N_u$ is large.

Finally, we should to point out that although theoretically the power gap of Q-CSIT and I-CSIT relative to F-CSIT tends to zero as $L, N_u \to \infty$, our numerical results suggest that even a few feedback bits (e.g., $L = 2^3$ and $N = 2^5$) suffice to close the gap.

*Test Case 5 (Sensitivity to Synchronization, i.e., Mistiming Effects):* Since the synchronization among sensors assumed under (as1) is challenging to obtain, we will rely on simulated tests to gauge how sensitive is our design to synchronization errors. Although systems with instantaneous CSI at both receiver and transmitter can cope with synchronization errors, here we test a worst case scenario where these errors are so fast that neither the receiver nor the nodes can account for them. The simulated setup consists of four sensors with random mistiming bounded by $\varepsilon$. On the one hand the FC is unable to estimate and compensate for these mistiming errors and thus quantizes the erro-

TABLE III
OPTIMUM AVERAGE POWER (IN DB) AND RATE LOADING PER AMC MODE (QUANTIZATION STATE) AND QUANTIZATION THRESHOLDS ($M = 4, r_0 = 2.5, \epsilon_0 = 10^{-3}, L = 4, r_l = [0, 1, 3, 5], N_u = 16$)

| | F-CSIT | | | I-CSIT | | | Q-CSIT | | |
|---|---|---|---|---|---|---|---|---|---|
| AMC mode | $l=2$ | $l=3$ | $l=4$ | $l=2$ | $l=3$ | $l=4$ | $l=2$ | $l=3$ | $l=4$ |
| Average Tx-Power: $\bar{p}_l$ | 4.96 | 9.57 | 11.75 | 4.40 | 10.64 | 14.62 | 7.02 | 11.45 | 13.54 |
| Tx-Rate: $r_l$ | 1 | 3 | 5 | 1 | 3 | 5 | 1 | 3 | 5 |
| Thresholds: $\tau_{l+1}$ | 0.8 | 2.4 | 9.7 | 1.7 | 3.0 | 5.8 | 0.6 | 1.6 | 5.1 |
| Probability: $\Pr\{l^* = l\}$ | 0.22 | 0.75 | 0.01 | 0.26 | 0.48 | 0.17 | 0.25 | 0.68 | 0.05 |

TABLE IV
AVERAGE TRANSMIT POWER (IN DB) AS $L$ VARIES

| $L$ | 1 | 2 | 4 | 6 | 8 | $\infty$ |
|---|---|---|---|---|---|---|
| F-CSIT | 9.8 | 9.4 | 8.6 | 8.5 | 8.4 | 8.3 |
| I-CSIT | 13.9 | 11.5 | 10.2 | 9.4 | 8.9 | 8.3 |
| Q-CSIT | 14.2 | 11.7 | 10.7 | 9.8 | 9.3 | 8.9 |

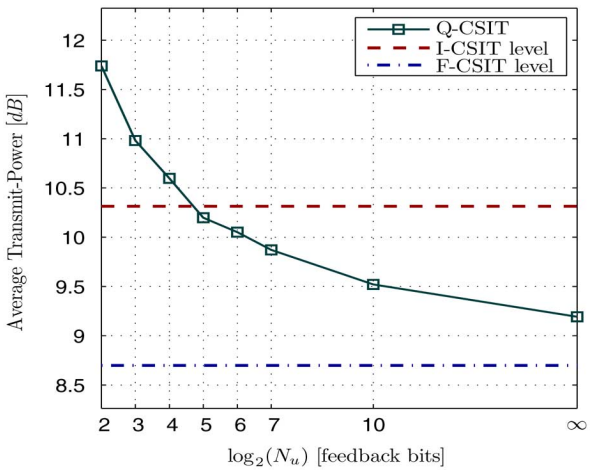


Fig. 3. Effect of number of feedback bits for Q-CSIT scheme ($M = 4$, $r_0 = 2.5, L = 4$).

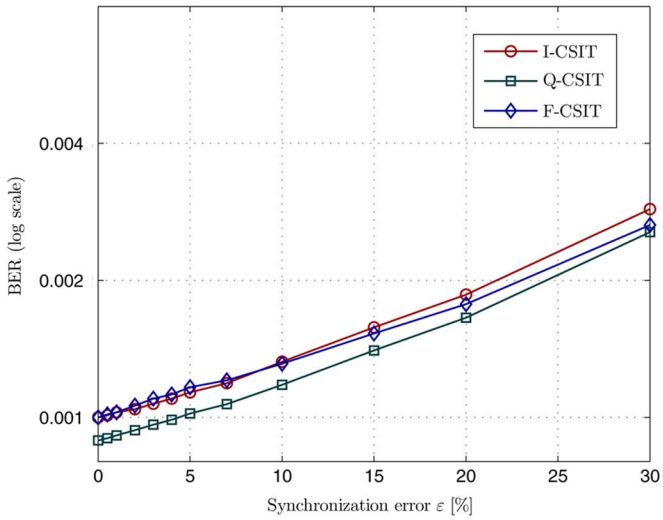


Fig. 4. BER degradation due to synchronization mistiming for F-CSIT, Q-CSIT and I-CSIT schemes ($M = 4, r_0 = 2.5, L = 4$).

neous channel gain. On the other hand, the sensors adapt their transmit configurations using codebooks designed considering perfect synchronization (thus, suboptimum in the presence of mistiming) and based on the erroneous information fed back by the FC.

Based on this setup, Fig. 4 depicts BER measured at the FC for different mistiming errors when the target rate and BER are 2.5 and $10^{-3}$, respectively, for the cases of F-CSIT, Q-CSIT and I-CSIT based operation. As expected, BER performance degrades when synchronization errors occur, increasing moderately for small values of $\varepsilon$ and exponentially for systems with very poor synchronization (average transmit power and rate are not presented since they remain unchanged with the FC not mitigating for mistiming). Focusing on the Q-CSIT case, we observe that this system exhibits the best BER performance. Specifically for timing errors not exceeding 5%, the system performs below the target BER and even for errors up to 20%, the BER in less than twice the required value. The reason for this behavior is twofold: i) our design is based on an upper bound [cf. (24)] which, although tight, yields a conservative design that slightly oversatisfies the BER requirement; and ii) the quantized CSIT naturally accounts for uncertainty in channel estimation making the design more robust synchronization errors. More important, Fig. 4 suggests that our novel adaptive schemes are robust to low-moderate timing synchronization errors.

## VII. CONCLUSION

In a WSN entailing coherent sensor communications with a fusion center, we minimized the average transmit power subject to average rate and BER requirements when full (F-) CSIT, quantized (Q-) CSIT or individual (I-) CSIT is available. With finite-rate feedback, we optimally separated the main design in two subproblems: i) MISO channel quantization and beamforming, and ii) rate/power quantization and allocation. By exploiting the parallelism between the coherent WSN setup and a distributed MISO system, we relied on nonlinear programming tools to solve the programs at hand and derived the corresponding power-efficient channel quantization and adaptive transmission policies. Numerical results confirmed that our limited-rate feedback (Q-CSIT and I-CSIT)-based solutions attain power efficiency surprisingly close to the optimal F-CSIT based

benchmark. They outperform a S-CSIT scheme which only exploits spatial diversity with F-CSIT, and offer significant power savings relative to open loop systems that do not exploit CSIT.

## APPENDIX A
## CLOSED-FORM BER EXPRESSION FOR Q-CSIT

Finding a closed-form expression for $\varphi_\epsilon(\tilde{\tau}_l, \tilde{\tau}_{l+1}, \tilde{p}_l, r_l, \epsilon_0)$ requires analytical evaluation of the two integrals involved in (29). Using the CDF of $g$, we have for the second integral that $\int_{\tilde{\tau}_l}^{\tilde{\tau}_{l+1}} f_{\tilde{g}}(\tilde{g})d\tilde{g} = \tilde{F}_{\tilde{g}}(\tilde{\tau}_{l+1}) - \tilde{F}_{\tilde{g}}(\tilde{\tau}_l)$. The first integral in (29) requires solving analytically $\tilde{\Phi}(p,r,x) := \int \epsilon(\tilde{g},p,r) f_{\tilde{g}}(\tilde{g})d\tilde{g}|_{\tilde{g}=x}$. Utilizing (9) with $b := \kappa_2 p/(2^r-1)$, the latter can be rewritten as $\tilde{\Phi}(p,r,x) = \kappa_1 \int \exp(-b\tilde{g}) f_{\tilde{g}}(\tilde{g})d\tilde{g}|_{\tilde{g}=x}$, which after tedious manipulations yields [cf. (26)]

$$\begin{aligned}
&\int \exp(-b\tilde{g}) f_{\tilde{g}}(\tilde{g})d\tilde{g} \\
&= \int \frac{1}{\Gamma(M)} \left\{ \exp\left(-\frac{1+b(1-z_{\max})}{1-z_{\max}}\tilde{g}\right) \right. \\
&\quad \times \frac{\tilde{g}^{M-1}}{(1-z_{\max})^M} \left(1 - N_u z_{\max}^M\right) + N_u \exp(-(1+b)\tilde{g}) \\
&\quad \left. \times \left[\Gamma(M) - \Gamma(M, z_{\max}\tilde{g}/(1-z_{\max}))\right] \right\} d\tilde{g} \\
&= \frac{-1}{\Gamma(M)[1+b]} \left\{ \frac{(1+b)\left(1 - N_u z_{\max}^M\right) + N_u z_{\max}^M}{[1+b(1-z_{\max})]^M} \right. \\
&\quad \times \Gamma\left(M, \tilde{g}\frac{1+b(1-z_{\max})}{1-z_{\max}}\right) + \frac{N_u \exp(-(1+b)\tilde{g})}{1+b} \\
&\quad \left. \times \left[\Gamma(M) - \Gamma(M, \tilde{g}z_{\max}/(1-z_{\max}))\right] \right\}. \qquad (40)
\end{aligned}$$

Based on (40), we can write (29) in closed-form as

$$\begin{aligned}
\varphi_\epsilon(\tilde{\tau}_l, \tilde{\tau}_{l+1}, \tilde{p}_l, r_l, \epsilon_0) =& \tilde{\Phi}(\tilde{p}_l, r_l, \tilde{\tau}_{l+1}) - \tilde{\Phi}(\tilde{p}_l, r_l, \tilde{\tau}_l) \\
&- \epsilon_0[\tilde{F}_{\tilde{g}}(\tilde{\tau}_{l+1}) - \tilde{F}_{\tilde{g}}(\tilde{\tau}_l)]. \qquad (41)
\end{aligned}$$

Finally, based on (28) and (41) we arrive at

$$\tilde{\epsilon}_l(\tilde{\tau}_l, \tilde{\tau}_{l+1}, \tilde{p}_l, r_l) = \frac{\tilde{\Phi}(\tilde{p}_l, r_l, \tilde{\tau}_{l+1}) - \tilde{\Phi}(\tilde{p}_l, r, \tilde{\tau}_l)}{\tilde{F}_{\tilde{g}}(\tilde{\tau}_{l+1}) - \tilde{F}_{\tilde{g}}(\tilde{\tau}_l)} \qquad (42)$$

which quantifies the average BER analytically when the proposed Q-CSIT design is in force.

## APPENDIX B
## CLOSED-FORM OF THE POWER DERIVATIVE BASED ON Q-CSIT

For the PDF of $\tilde{g}$ in (26), we can write

$$\int_{\tilde{\tau}_i}^{\tilde{\tau}_{i+1}} [\partial\epsilon(\tilde{g},p,r)/\partial p] f_{\tilde{g}}(\tilde{g})d\tilde{g} = \tilde{\xi}(p,r,\tilde{\tau}_{i+1}) - \tilde{\xi}(p,r,\tilde{\tau}_i). \quad (43)$$

Differentiating (9) w.r.t. $p$, we can rewrite (43) as

$$\begin{aligned}
\tilde{\xi}(p,r,x) &:= \int [\partial\epsilon(\tilde{g},p,r)/\partial p] f_{\tilde{g}}(\tilde{g})d\tilde{g}|_{\tilde{g}=x} \\
&:= \frac{-\kappa_1\kappa_2}{2^r-1} \tilde{I}_\xi\left(\frac{\kappa_2 p}{2^r-1}, \tilde{g}\right)\Big|_{\tilde{g}=x} \qquad (44)
\end{aligned}$$

where $\tilde{I}_\xi(b,g)$ is found in closed-form as

$$\begin{aligned}
&\tilde{I}_\xi(b,\tilde{g}) \\
&:= \int \tilde{g}\exp(-b\tilde{g}) f_{\tilde{g}}(\tilde{g})d\tilde{g} \\
&= \int \frac{1}{\Gamma(M)} \left\{ \exp\left(-\frac{1+b(1-z_{\max})}{1-z_{\max}}\tilde{g}\right) \frac{\tilde{g}^M}{(1-z_{\max})^M} \right. \\
&\quad \times \left(1 - N_u z_{\max}^M\right) + N_u \exp(-(1+b)\tilde{g}) \\
&\quad \left. \times \left[\Gamma(M) - \Gamma(M, z_{\max}\tilde{g}/(1-z_{\max}))\right]\tilde{g} \right\} d\tilde{g} \\
&= \frac{-1}{\Gamma(M)} \left\{ (1-z_{\max}) \frac{1 - N_u z_{\max}^M}{[1+b(1-z_{\max})]^{M+1}} \right. \\
&\quad \times \Gamma\left(M+1, \tilde{g}\frac{1+b(1-z_{\max})}{1-z_{\max}}\right) \\
&\quad + \frac{N_u \exp(-(1+b)\tilde{g})(1+(1+b)\tilde{g})}{(1+b)^2} \\
&\quad \times \left[\Gamma(M) - \Gamma(M, \tilde{g}z_{\max}/(1-z_{\max}))\right] \\
&\quad + \frac{N_u z_{\max}^M}{(1+b)^2[1+b(1-z_{\max})]^{M+1}} \\
&\quad \times \left[1 + b(1-z_{\max})\Gamma\left(M, \tilde{g}\frac{1+b(1-z_{\max})}{1-z_{\max}}\right)\right. \\
&\quad \times (1+b)(1-z_{\max}) \\
&\quad \left. \left. \times \Gamma\left(M+1, \tilde{g}\frac{1+b(1-z_{\max})}{1-z_{\max}}\right)\right] \right\}. \qquad (45)
\end{aligned}$$

## ACKNOWLEDGMENT

The views and conclusions contained in this document are those of the authors and should not be interpreted as representing the official policies, either expressed or implied, of the Army Research Laboratory or the U.S. Government.

## REFERENCES

[1] I. F. Akyildiz, W. Su, Y. Sankarsubramaniam, and E. Cayirci, "Wireless sensor networks: A survey," *Comput. Netw.*, vol. 38, pp. 393–422, Mar. 2002.

[2] J. N. Al-Karaki and A. E. Kamal, "Routing techniques in wireless sensor networks: A survey," *IEEE Wireless Commun. Mag.*, vol. 11, no. 6, pp. 6–28, Dec. 2004.

[3] W. U. Bajwa, A. M. Sayeed, and R. Nowak, "Matched source-channel communication for field estimation in wireless sensor networks," in *Proc. Int. Conf. Inf. Process. Sensor Networks*, Los Angeles, CA, Apr. 2005, pp. 332–339.

[4] G. Barriac, R. Mudumbai, and U. Madhow, "Distributed beamforming for information transfer in sensor networks," in *Proc. Int. Symp. Inf. Process. Sensor Networks*, Berkeley, CA, Apr. 2004, pp. 81–88.

[5] D. Bertsekas, *Nonlinear Programming*, 2nd ed. Belmont, MA: Athena Scientific, 1999.

[6] M. Bhardwaj, T. Garnett, and A. P. Chandrakasan, "Upper bounds on the lifetime of sensor networks," in *Proc. Int. Conf. Commun.*, Helsinki, Finland, Jun. 2001, vol. 3, pp. 785–790.
[7] S. Boyd and L. Vandenberghe, *Convex Optimization*. Cembridge, U.K.: Cambridge Univ. Press, 2004.
[8] J. H. Conway, R. H. Hardin, and N. J. A. Sloane, "Packing lines, planes, etc.: Packings in Grassmannian space," *Exp. Math.*, vol. 5, no. 2, pp. 139–159, 1996.
[9] G. B. Giannakis, Z. Liu, X. Ma, and S. Zhou, *Space-Time Coding for Broadband Wireless Communications*. New York: Wiley, 2007.
[10] A. Goldsmith, *Wireless Communications*. Cambridge, U.K.: Cambridge Univ. Press, 2005.
[11] A. J. Goldsmith and S. G. Chua, "Adaptive coded modulation for fading channels," *IEEE Trans. Commun.*, vol. 46, no. 5, pp. 595–602, May 1998.
[12] J. F. Hayes, "Adaptive feedback communications," *IEEE Trans. Commun.*, vol. 16, no. 1, pp. 29–34, Feb. 1968.
[13] A. Lapidoth and S. Shamai, "Fading channels: How perfect need perfect side information be?," *IEEE Trans. Inf. Theory*, vol. 48, no. 5, pp. 1118–1134, May 2002.
[14] L. Lin, R. Yates, and P. Spasojević, "Adaptive transmission with discrete code rates and power levels," *IEEE Trans. Inf. Theory*, vol. 51, no. 12, pp. 2115–2125, Dec. 2003.
[15] D. J. Love, Grassmannian Subspace Packing [Online]. Available: http://cobweb.ecn.purdue.edu/~djlove/grass.html [Online] Available
[16] D. J. Love, R. W. Heath Jr., and T. Ströhmer, "Grassmannian beamforming for multiple-input multiple-output wireless systems," *IEEE Trans. Inf. Theory*, vol. 49, no. 10, pp. 2735–2747, Oct. 2003.
[17] X. Luo and G. B. Giannakis, "Raise your voice at a proper pace to synchronize in multiple ad hoc piconets," *IEEE Trans. Signal Process.*, vol. 55, no. 1, pp. 267–278, Jan. 2007.
[18] A. G. Marques, F. F. Digham, and G. B. Giannakis, "Optimizing power efficiency of OFDM using quantized channel state information," *IEEE J. Sel. Areas Commun.*, vol. 24, no. 8, pp. 1581–1592, Aug. 2006.
[19] A. G. Marques, X. Wang, and G. B. Giannakis, "Optimizing energy efficiency of TDMA with finite rate feedback," in *Proc. Int. Conf. Acoust., Speech, Signal Process*, Honolulu, HI, Apr. 2007, vol. 3, pp. 117–120.
[20] K. Mukkavilli, A. Sabharwal, E. Erkip, and B. Aazhang, "On beamforming with finite-rate feedback in multiple-antenna systems," *IEEE Trans. Inf. Theory*, vol. 49, no. 10, pp. 2562–2579, Oct. 2003.
[21] K. Simon and M. S. Alouini, "Exponential-type bounds on the generalized Marcum Q-function application to error probability analysis over fading channels," *IEEE Trans. Commun.*, vol. 48, no. 3, pp. 359–366, Mar. 2000.
[22] J. Wu, S. Zhou, Z. Wang, and M. Doroslovacki, "Quantifying the performance gain of direction feedback in a MISO system," in *Proc. Conf. Info. Sciences Systems*, Princeton, NJ, Mar. 2006.
[23] J.-J. Xiao, S. Cui, Z.-Q. Luo, and A. J. Goldsmith, "Power scheduling of universal decentralized estimation in sensor networks," *IEEE Trans. Signal Process.*, vol. 54, no. 2, pp. 413–422, Feb. 2006.
[24] W. Ye, J. Heidemann, and D. Estrin, "An energy-efficient MAC protocol for wireless sensor networks," in *Proc. 21st Annu. Joint Conf. IEEE Computer Commun. Societies*, New York, Jun. 2002, vol. 3, pp. 1567–1576.
[25] S. Zhou and B. Li, "BER criterion and codebook construction for finite-rate precoded spatial multiplexing with linear receivers," *IEEE Trans. Signal Process.*, vol. 54, no. 5, pp. 1653–1665, May 2006.
[26] S. Zhou, Z. Wang, and G. B. Giannakis, "Quantifying the power-loss when transmit-beamforming relies on finite-rate feedback," *IEEE Trans. Wireless Commun.*, vol. 4, no. 3, pp. 1948–1957, Jul. 2005.

**Antonio G. Marques** (M'07) received the Telecommunication Engineering degree and the Doctorate degree (together equivalent to the B.Sc., M.Sc., and Ph.D. degrees in electrical engineering), both with highest honors, from the Universidad Carlos III de Madrid, Madrid, Spain, in 2002 and 2007, respectively.

In 2003, he joined the Department of Signal Theory and Communications, Universidad Rey Juan Carlos, Madrid, Spain, where he currently develops his research and teaching activities as an Assistant Professor. Since 2005, he has also been a Visiting Researcher at the Department of Electrical Engineering, University of Minnesota, Minneapolis. His research interests lie in the areas of communication theory, signal processing, and networking. His current research focuses on channel state information designs, energy-efficient resource allocation, and wireless ad hoc and sensor networks.

Dr. Marques received several awards for his work in distinctive international conferences, including the International Conference on Acoustics, Speech and Signal Processing (ICASSP) 2007.

**Xin Wang** (M'04) received the B.Sc. degree and the M.Sc. degree from Fudan University, Shanghai, China, in 1997 and 2000, respectively, and the Ph.D. degree from Auburn University, Auburn, IL, in 2004, all in electrical engineering.

From September 2004 to August 2006, he was a Postdoctoral Research Associate with the Department of Electrical and Computer Engineering, University of Minnesota, Minneapolis. Since September 2006, he has been an Assistant Professor in the Department of Electrical Engineering, Florida Atlantic University, Boca Raton. His research interests include medium access control, cross-layer design, resource allocation, and signal processing for communication networks.

**Georgios B. Giannakis** (F'97) received the Diploma degree in electrical engineering from the National Technical University of Athens, Greece, in 1981. From 1982 to 1986, he was with the University of Southern California (USC), where he received the M.Sc. degree in electrical engineering in 1983, the M.Sc. degree in mathematics in 1986, and the Ph.D. degree in electrical engineering in 1986.

Since 1999, he has been a Professor with the Electrical and Computer Engineering Department at the University of Minnesota, where he now holds an ADC Chair in wireless telecommunications. His general interests span the areas of communications, networking and statistical signal processing—subjects on which he has published more than 275 journal papers, 450 conference papers, two edited books, and two research monographs. Current research focuses on complex-field and network coding, multicarrier, cooperative wireless communications, cognitive radios, cross-layer designs, mobile ad hoc networks, and wireless sensor networks.

Dr. Giannakis is the (co-)recipient of six paper awards from the IEEE Signal Processing (SP) and Communications Societies, including the G. Marconi Prize Paper Award in wireless communications. He also received Technical Achievement Awards from the SP Society (2000), from EURASIP (2005), a Young Faculty Teaching Award, and the G. W. Taylor Award for Distinguished Research from the University of Minnesota. He has served the IEEE in a number of posts, and is currently a Distinguished Lecturer for the IEEE SP Society.